

Discovery of a strong Baldwin effect in mid-infrared AGN lines[★]

S. F. Hönig¹, A. Smette², T. Beckert¹, H. Horst^{3,4}, W. Duschl³, P. Gandhi⁵, M. Kishimoto¹, and G. Weigelt¹

¹ Max-Planck-Institut für Radioastronomie, Auf dem Hügel 69, 53121 Bonn, Germany

² European Southern Observatory, Casilla 19001, Santiago 19, Chile

³ Institut für Theoretische Physik und Astrophysik, Christian-Albrechts-Universität zu Kiel, Leibnizstr. 15, 24098 Kiel, Germany

⁴ Zentrum für Astronomie, ITA, Universität Heidelberg, Albert-Ueberle-Str. 2, 69120 Heidelberg, Germany

⁵ RIKEN Cosmic Radiation Lab, 2-1 Hirosawa, Wakoshi Saitama 351-0198, Japan

Received 5 May 2008 / Accepted 14 May 2008

ABSTRACT

We present the discovery of a Baldwin effect in 8 nearby Seyfert galaxies for the three most prominent mid-infrared forbidden emission lines observable from the ground that are commonly found in AGN, [Ar III]($\lambda 8.99 \mu\text{m}$), [S IV]($\lambda 10.51 \mu\text{m}$), and [Ne II]($\lambda 12.81 \mu\text{m}$). The observations were carried out using the VLT/VISIR imager and spectrograph at the ESO/Paranal observatory. The bulk of the observed line emission comes from the inner <0.4 which corresponds to spatial scales <100 pc in our object sample. The correlation index is approximately -0.6 without significant difference among the lines. This is the strongest anti-correlation between line equivalent width and continuum luminosity found so far. In the case of Circinus, we show that despite the use of mid-infrared lines, obscuration by either the host galaxy or the circumnuclear dust torus might affect the equivalent widths. Given the small observed spatial scales from which most of the line emission emanates, it is unclear how these observations fit into the favored “disappearing NLR” scenario for the narrow-line Baldwin effect.

Key words. Galaxies: Seyfert – Galaxies: nuclei – Infrared: galaxies – quasars: emission lines – X-rays: galaxies

1. Introduction

The Baldwin effect, a negative correlation between equivalent width, W_λ , and continuum luminosity, L , is commonly found in broad UV/optical emission lines of AGN. Initially, it was reported for the C IV($\lambda 1549$) line (Baldwin 1977) for which $W_\lambda \propto L^{-0.2}$, but later also found in emission lines of many other species for which the strength of the correlation depends on the ionization potential of the respective line (e.g. Dietrich et al. 2002). Although the Baldwin effect is well established, its physical origin is still a matter of debate. A common explanation refers to the spectral shape of the ionizing continuum which appears softer in high luminosity sources than in AGN with lower luminosities. This results in a relatively lower number of ionizing photons in the broad-line region (BLR) which, in turn, leads to a smaller W_λ . While this explanation is, at least, qualitatively in agreement with the observed dependence on line ionization energy, it is not clear if L is the fundamental parameter that drives the broad-line Baldwin effect (BLBE). Instead, a similar effect has been observed if L is replaced by the black hole mass, M_{BH} , or the Eddington ratio, $l_{\text{Edd}} = L/L_{\text{Edd}}$ (e.g. Wandel 1999; Warner et al. 2004).

In addition to the BLBE, several narrow optical emission lines have been found to show a Baldwin effect with similar order-of-magnitude luminosity-dependence as well (hereafter: oNLBE; e.g. Brorsen & Green 1992; McIntosh et al. 1999; Croom et al. 2002). Given the different spatial scales where the broad- and the narrow-lines are emitted, it is generally believed that the driving physical mechanisms for the BLBE and oNLBE

are different (e.g. Shields 2007, and references therein). A luminosity-dependence of the equivalent width, sometimes referred to as Iwasawa-Taniguchi effect, is also known for the narrow $K\alpha$ -line in X-rays (e.g. Iwasawa & Taniguchi 1993; Bianchi et al. 2007).

In this letter, we present our discovery of a strong Baldwin effect in nearby Seyfert galaxies for the most prominent narrow emission lines that are present in AGN mid-infrared spectra and observable from the ground, in particular [Ar III]($\lambda 8.99 \mu\text{m}$), [S IV]($\lambda 10.51 \mu\text{m}$), and [Ne II]($\lambda 12.81 \mu\text{m}$). The Baldwin Effect in these mid-infrared forbidden lines (hereafter: iNLBE) is much stronger than for any other as yet observed. In Sect 2, we report on details about the VLT/VISIR observations. In Sect. 3, the results are presented, followed by a discussion of our finding in Sect. 4. This paper (hereafter: paper I) presents first results on line emission of our larger campaign using VLT/VISIR which is dedicated to mid-infrared spectroscopy of nearby AGN at high spatial resolution. A forthcoming paper (hereafter: paper II) will deal with the mid-infrared continuum emission of AGN. In the following, we will use cosmological parameters $H_0 = 73$ km/(s Mpc), $\Omega_\Lambda = 0.72$, and $\Omega_m = 0.24$ (Spergel et al. 2007).

2. Observations

We used the mid-infrared imager and spectrograph VISIR located at the 8 m UT3 telescope of the ESO/Paranal observatory. With VISIR, we observed a sample of 8 nearby AGN of which 5 are Seyfert 2 (S1h, S1i, S2) and 3 are Seyfert 1 (S1.0, S1.5) galaxies. The 8 – 13 μm N -band spectra were acquired in low spectral resolution mode ($R \sim 300$), for which 4 different wavelength settings centered at 8.5, 9.8, 11.4, and 12.4 μm have to be combined for each object. With VISIR, the achieved spatial

Send offprint requests to: S. F. Hönig
e-mail: shoening@mpi.fr-bonn.mpg.de

[★] Based on ESO observing programmes 078.B-0303, 080.B-0240, and the DDT program 280.B-5068.

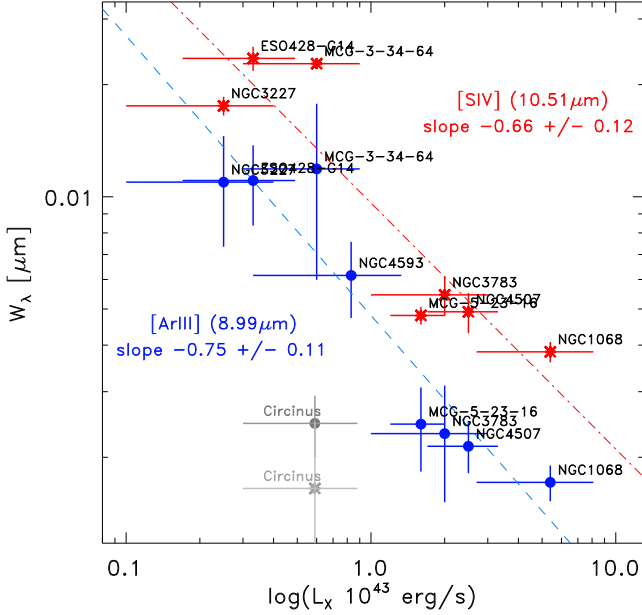


Fig. 1. Equivalent width, W_λ , of the [Ar III] (blue circles) and [S IV] (red crosses) lines plotted over the X-ray luminosity, L_X , for our sample of nearby AGN as listed in Table 1. The fitted correlations $W_\lambda \propto L_X^{-0.75 \pm 0.11}$ for [Ar III] (blue dashed line; $\rho_{\text{Spearman}} = -0.91$, significance 0.002), and $W_\lambda \propto L_X^{-0.66 \pm 0.12}$ for [S IV] (red dashed-dotted line; $\rho_{\text{Spearman}} = -0.79$, significance 0.04) are shown. Circinus (gray symbols) is outlying probably due to significant obscuration by dust in the host galaxy or the circumnuclear dust torus (see Fig. 4).

resolution in this wavelength range is $0''.25 - 0''.39$, which is a factor 2 – 4 smaller than the used slit widths of $0''.75 - 1''.0$ making slit losses negligible. The resulting spectra were extracted using the standard VISIR CPL pipeline (V3.0.0) and calibrated by a number of generic standard stars. For NGC 4507, a single standard star observed within the same night has been used for calibration. In addition to the 8 objects, archival VISIR data of NGC 1068 and NGC 253 has been downloaded, extracted, and calibrated in the same way. A more detailed description of the observations will be presented in paper II. NGC 4593 has been observed only in the 8.5 and 9.8 μm settings, corresponding to a restframe wavelength coverage of approximately 7.9 – 10.4 μm . As a result, only [Ar III] ($\lambda 8.99 \mu\text{m}$) is seen in the combined spectrum, giving W_λ data in this line on a total of 8 objects. For [S IV] ($\lambda 10.51 \mu\text{m}$), and [Ne II] ($\lambda 12.81 \mu\text{m}$), equivalent widths of 7 objects is available.

3. The Baldwin effect in forbidden mid-IR lines

3.1. Results

In Table 1, we present extracted W_λ of all three lines. For all objects, the line emission was strongly peaked towards the nucleus. Except for the emission in the most nearby objects NGC 1068 ($\sim 10\%$ extension in [S IV] with respect to the continuum PSF) and Circinus ($\sim 50\%$ extension in [S IV] and [Ne II]), no spatial extension was detected in the continuum and the lines. The reduction was done in a way that even for these extended objects, almost no line flux is lost by the extraction window. The errors on W_λ represent the uncertainty due to the determination of the

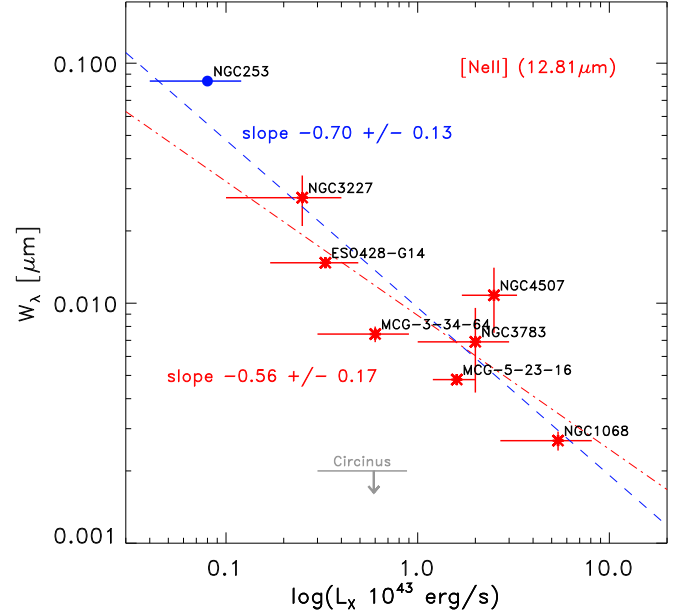


Fig. 2. Equivalent width, W_λ , of the [Ne II] line plotted over the X-ray luminosity, L_X for 7 nearby Seyfert galaxies (red crosses). The fitted correlation $W_\lambda \propto L_X^{-0.56 \pm 0.17}$ ($\rho_{\text{Spearman}} = -0.75$, significance 0.05), is shown as red, dashed-dotted line. When including NGC 253 (blue circle) – despite its questionable AGN nature – a correlation $W_\lambda \propto L_X^{-0.70 \pm 0.13}$ ($\rho_{\text{Spearman}} = -0.83$, significance 0.01) is found (blue dashed line). An upper limit for Circinus (gray arrow) is given. The non-detection of [Ne II] from the nuclear point source is probably due to significant obscuration by dust in the host galaxy or the circumnuclear dust torus (see Fig. 4).

shape of continuum emission underlying the emission line. This uncertainty is in part due to the presence of sky lines in those spectra which were taken under unfavorable atmospheric conditions (e.g. high amount of precipitable water vapor). This affects the [Ne II] line the most since strong atmospheric bands are present between 12.4 – 12.7 μm . On the other hand, the error bars of the [Ar III] line are predominantly caused by the general weakness of the line with respect to the continuum.

In addition to the line W_λ s, Table 1 lists (absorption-corrected) 2 – 10 keV X-ray luminosities, L_X , for our sample of AGN. These are taken as a measure for the ionizing continuum luminosity since the UV/optical AGN emission of our type 2 sources is heavily affected by dust absorption from the putative circumnuclear dust torus. Unfortunately, 3 of our objects are Compton-thick to the X-ray emission (NGC 1068, Circinus, and ESO 428–G14). For these objects, we estimated the nuclear X-ray luminosity by extracting the 12 μm continuum emission from our spectra, which will be presented in paper II, and translating the corresponding spectral luminosity into L_X using the most recent version of the $L_{\text{MIR}} - L_X$ -correlation for AGN as established from VISIR observations with similar spatial resolution (Horst et al. 2008). We adopt 50% of error on L_X for these objects.

In Figs. 1 & 2, we show the measured W_λ of [Ar III], [S IV], and [Ne II] versus L_X . The trend of smaller W_λ with luminosity is evident. As an illustration, the spectral regions around the [Ar III] and [S IV] lines are presented in Fig. 3 for NGC 3227 ($\log L_X = 42.4$), MCG–5–23–16 ($\log L_X = 43.2$), and NGC 1068 ($\log L_X =$

Table 1. Equivalent widths and X-ray luminosities of our sample of nearby AGN.

| object | type ^a | D_L ^b (Mpc) | $10\ \mu\text{m}$ scale ^c (pc) | W_λ ([Ar III]) ($10^{-4}\ \mu\text{m}$) | W_λ ([S IV]) ($10^{-4}\ \mu\text{m}$) | W_λ ([Ne II]) ($10^{-4}\ \mu\text{m}$) | L_X (10^{43} erg/s) | ref. |
|-------------|-------------------|-----------------------------|--|--|--|---|-----------------------------|------|
| NGC 1068 | S1h | 14.4 ^d | 21.4 | 17.13 ± 0.94 | 38.37 ± 1.21 | 26.74 ± 1.21 | 5.4 ± 2.7 | 1 |
| ESO 428-G14 | S2 | 22.3 | 33.2 | 110.57 ± 13.43 | 235.16 ± 8.74 | 147.40 ± 2.44 | 0.33 ± 0.16 | 1 |
| MCG-5-23-16 | S1i | 39.5 | 58.8 | 24.55 ± 3.12 | 48.04 ± 1.30 | 111.61 ± 1.46 | 1.7 ± 1.0 | 2 |
| NGC 4507 | S1h | 54.5 | 80.9 | 21.41 ± 1.64 | 49.14 ± 3.03 | 107.91 ± 16.32 | 2.5 ± 0.8 | 3 |
| Circinus | S1h | 4.2 ^e | 6.2 | 24.66 ± 2.31 | 16.50 ± 4.20 | < 27 | 0.59 ± 0.29 | 1 |
| MCG-3-34-64 | S1h | 63.3 | 94.2 | 118.78 ± 29.46 | 227.63 ± 1.28 | 74.35 ± 2.77 | 0.6 ± 0.3 | 3 |
| NGC 3783 | S1.5 | 44.7 | 66.5 | 23.15 ± 4.00 | 54.56 ± 3.33 | 68.99 ± 13.28 | 2.0 ± 1.0 | 3 |
| NGC 3227 | S1.5 | 20.4 | 30.4 | 109.48 ± 18.02 | 175.37 ± 5.09 | 275.10 ± 32.69 | 0.25 ± 0.15 | 4 |
| NGC 4593 | S1.0 | 42.0 | 62.5 | 61.52 ± 7.19 | ... | ... | 0.83 ± 0.50 | 5 |
| NGC 253 | S | 3.5 ^f | 5.2 | ... | ... | 842.27 ± 11.13 | 0.08 ± 0.04 | 1 |

— Notes: ^a AGN types from Veron-Cetty & Veron (2006); ^b Luminosity distance based on CMB reference frame redshifts from NED, otherwise indicated; ^c Diffraction limit for a 8.2 m VLT telescope $\sim 0''.25$; ^d Tully (1988); ^e Freeman et al. (1977); ^f Rekola et al. (2005)
— References: (1) $L_{\text{MIR}} - L_X$ -correlation from Horst et al. (2008) using $12\ \mu\text{m}$ VISIR fluxes for NGC 1068 (14 Jy), Circinus (10 Jy), ESO 428-G14 (0.22 Jy), and NGC 253 (2.1 Jy); (2) Balestra et al. (2004); (3) Horst et al. (2008); (4) mean of recent 2–10 keV (Cappi et al. 2006) and 17–60 keV (Sazanov et al. 2007) data taken, 60% error inferred due to variability; (5) Shinozaki et al. (2006)

43.7). A statistical analysis of the correlation for our sample shows Spearman ranks $\rho_{\text{Spearman}} = -0.75 \dots -0.9$ with significance levels in the range of $0.2 - 5 \times 10^{-2}$. Despite the limited number of objects and luminosity coverage, correlations evolving out of the data can be confidently established. For BLBE and oNLBE studies, higher significance is achieved by averaging spectra of different objects within a narrow luminosity range. This overcomes peculiarities of individual objects (e.g. Croom et al. 2002). We aim for observations of a larger sample to make similar studies for the presented iNLBE. It is important to note that no correlation of W_λ with AGN distance, D_L , is present in our sample ($\rho_{\text{Spearman}} < 0.25$, significance > 0.6 for all lines).

As of yet, only one other study mentions a possible Baldwin effect in the mid-infrared. In an AAS abstract, Keremedjiev & Hao (2006) presented the detection of a Baldwin effect for the [S IV] line in AGN data obtained by the *Spitzer* satellite. They also note indications of a Baldwin effect for [Ne II], admitting that their study is suffering from the low spatial resolution of the *Spitzer* data that they used. In the available abstract, nothing is mentioned about a slope or the scatter of the anti-correlation. Here, we demonstrate that the Baldwin effect of both the [S IV] and [Ne II] line, and in addition the [Ar III] line, is quite significant – and strong – when using high spatial resolution data, even with a small object sample. Thus, high spatial resolution appears to be crucial.

3.2. Relation to M_{BH} and l_{Edd}

For the three type 1 AGN in our sample, black hole masses, M_{BH} , have been estimated based on reverberation mapping data. We adopt black hole masses for NGC 3227 ($\log M_{\text{BH}}(M_\odot) = 7.63 \pm 0.31$) and NGC 3783 ($\log M_{\text{BH}} = 7.47 \pm 0.08$) from Onken et al. (2004), and $\log M_{\text{BH}} = 6.99 \pm 0.10$ for NGC 4593 from Denney et al. (2006). In addition, the black hole mass of the Seyfert 2 galaxy NGC 1068 could be determined by MASER cloud kinematics as $\log M_{\text{BH}} \approx 7.0$ (Greenhill et al. 1996). For these four AGN, we analyzed the dependence of the equivalent widths of the [Ar III] line on M_{BH} . A statistical test shows no evident correlation for our limited sample of objects and the small coverage of black hole masses ($\rho_{\text{Spearman}} = 0.40$, significance 0.6, for a nominal fit $W_\lambda([\text{Ar III}]) \propto M_{\text{BH}}^{0.5 \pm 0.7}$). Subject to the limi-

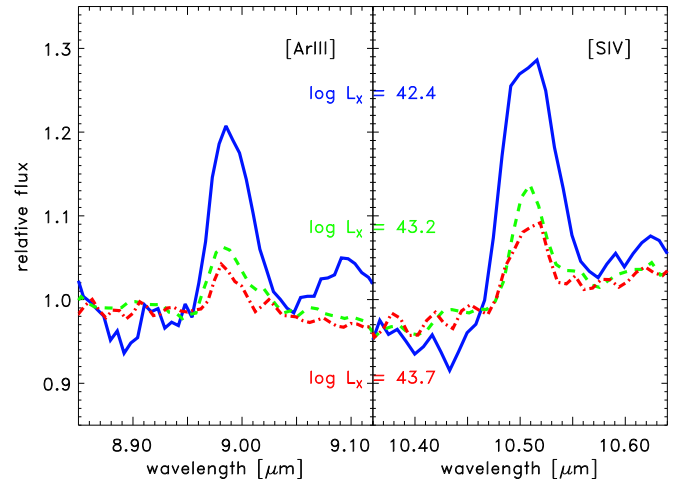


Fig. 3. [Ar III] (left) and [S IV] (right) spectral region of NGC 3227 ($\log L_X = 42.4$; solid blue line), MCG-5-23-16 ($\log L_X = 43.2$; dashed green line), and NGC 1068 ($\log L_X = 43.7$; dash-dotted red line) illustrating the decrease of W_λ with X-ray luminosity. The spectra have been smoothed to flatten the continuum.

tations, this indicates a fundamental difference of the iNLBE as compared to the BLBE for which such an anti-correlation has been found (Warner et al. 2004).

By using bolometric correction to the X-ray luminosities listed in Table 1 (Marconi et al. 2004), it is possible to estimate the Eddington ratio, l_{Edd} , of four AGN with known M_{BH} . A statistical test for a correlation between $W_\lambda([\text{Ar III}])$ and l_{Edd} reveals a Spearman rank $\rho_{\text{Spearman}} = -0.8$ with a significance of 0.2 for the relation $W_\lambda([\text{Ar III}]) \propto l_{\text{Edd}}^{-0.40 \pm 0.17}$. Thus, our limited sample doesn't allow us to firmly establish a correlation, but a negative dependence of W_λ on l_{Edd} is indicated.

3.3. The case of Circinus

We excluded Circinus from all analysis of the correlations. As can be seen in Figs. 1 & 2, the W_λ 's of all three mid-infrared lines deviate significantly from the nominal fit to the other AGN.

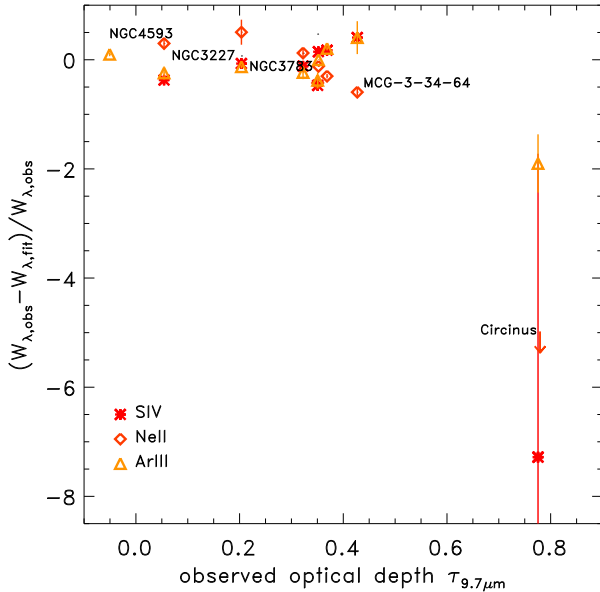


Fig. 4. Relative deviation of the observed W_λ from the correlation for all three lines plotted against the observed optical depth, $\tau_{9.7\mu\text{m}}$, in the silicate feature. Circinus, which is an outlier in the Baldwin correlations of all three lines, is the object with the deepest silicate feature. Due to radiative transfer effects, the actual obscuration of the central AGN by dust from the putative torus might be even stronger than suggested by the $\tau_{9.7\mu\text{m}}$ value.

Although it could be a resolution effect (Circinus is the nearest AGN in the sample), NGC 1068 has about the same spatial resolution when scaled for the different luminosities (scaling $r \propto L^{1/2}$). Moreover, we did not detect extended emission in the lines down to $\sim 5\%$ of the peak flux. This gives us some confidence to reject that a significant amount of line flux is over-resolved and lost in the noise.

Circinus is known for strong dust extinction towards the nucleus by dust lanes in both the host and our own Galaxy. In Fig. 4, we plot the deviation from the nominal correlation with X-ray luminosity (as given in Figs. 1 & 2) of each line against the depth of the silicate feature. Circinus shows the strongest deviations from all correlations and, at the same time, has the deepest silicate feature. It is deeper than in any other type 2 AGN in our sample. In case of foreground extinction (host or our galaxy), we expect that the flux within the lines is reduced in the same way without a change in W_λ . On the other hand, if part or all of the line emission is originating from inward of the torus, the extinction in the lines could be much stronger in a more or less edge-on torus geometry. Given the fact that the bulk of line emission in all other AGN is coming from the unresolved point source, such a scale and inclination effect appears possible. Strong extinction towards the NLR based on mid-infrared spectra of Circinus was also noted by Roche et al. (2006).

4. Discussion and conclusions

4.1. A comparison to UV/optical lines

The negative correlations in the [Ar III], [S IV], and [Ne II] lines as observed with VLT/VISIR is much stronger than any known Baldwin effect in optical/UV broad or narrow lines. This is remarkable since the spatial resolution in the optical of the most recent studies should be similar or even better than what is

achieved in the mid-infrared with the VLT. In UV/optical lines, a trend for larger correlation slopes with increasing ionization potential is observed (e.g. Dietrich et al. 2002). The potential of the presented lines is in the range of 40–47 eV and, thus, comparable to some of the optical/UV lines. From the optical/UV lines, slopes of the order of -0.1 to -0.2 would be expected. The measured slope of the mid-infrared lines deviates by at least $4\text{-}\sigma$ from that expectation (except [Ne II] w/o NGC 253: $2\text{-}\sigma$).

In Sect 3.2, we found some negative trend of W_λ ([Ar III]) with l_{Edd} , but possibly not with M_{BH} . If confirmed, this is in contrast to the observed and theoretically-expected behavior of the broad lines (e.g. Wandel 1999; Warner et al. 2004). Thus, the unsettled correlation with M_{BH} might imply that the iNLBE has a different physical origin than the BLBE, in particular questioning the relevance of the M_{BH} -dependence of the ionising continuum on the mid-infrared narrow-line emission.

4.2. Implications for the origin of the iNLBE

One suggestion for the origin of the oNLBE relates to the size scaling of the narrow-line region (NLR), for which a luminosity dependence $R_{\text{NLR}} \propto L^{0.5}$ has been found (Bennert et al. 2002). As a consequence, the NLR of luminous sources may reach galactic size scales and, thus, lose its gas. This scenario is often referred to as the “disappearing NLR” (Croom et al. 2002; Netzer et al. 2006). For the mid-infrared lines, we find that the main portion of their emission is not coming from a spatially-extended region, e.g. as for [O III] in the optical, but from scales smaller than 100 pc. If the lack of line emission in Circinus is really an inclination-dependent obscuration effect, then the involved scales are significantly smaller. Since it is difficult to imagine how the NLR could disappear on these scales, the iNLBE probably requires a different explanation. This explanation needs to explain, in particular, (1) the steepness of the correlation of the presented lines, and (2) the fact that the mid-infrared lines do not follow the ionisation potential-dependence as observed in optical lines. Possible mechanisms might involve a luminosity-dependent increase of density in the inner NLR (thus suppressing forbidden line emission).

Acknowledgements. We thank L. Spinoglio for helpful comments and suggestions which improved the paper. This research made use of the NASA/IPAC Extragalactic Database (NED) operated by the JPL (Caltech), under contract with NASA. PG is supported by JSPS and RIKEN Foreign postdoctoral fellowships. HH acknowledges support by DFG via SFB 439.

References

- Baldwin, J. A. 1977, ApJ, 214, 679
- Balestra, I., Bianchi, S., Matt, G. 2004, A&A, 415, 437
- Bennert, N., Falcke, H., Schulz, H., Wilson, A., Wills, B. J. 2002, ApJ, 574, L105
- Bianchi, S., Guainazzi, M., Matt, G., Fonseca Bonilla, N. 2007, A&A, 467, L19
- Brorsen, T. A., & Green, R. F. 1992, ApJS, 80, 109
- Cappi, M., Panessa, F., Bassani, L., et al. 2006, A&A, 446, 459
- Croom, S. M., Rhook, K., Corbett, E. A., et al. 2002, MNRAS, 337, 275
- Denney, K. D., Bentz, M. C., Peterson, B. M., et al. 2006, ApJ, 653, 152
- Dietrich, M., Hamann, F., Shields, J. C., et al. 2002, ApJ, 581, 912
- Freeman, K. C., Karlson, B., Lynga, J. F., et al. 1977, A&A, 55, 445
- Greenhill, L. J., Gwinn, C. R., Antonucci, R., Barvainis, R. 1996, ApJ, 472, L21
- Horst, H., Gandhi, P., Smette, A., Duschl, W. J. 2008, A&A, 479, 389
- Iwasawa, K., & Taniguchi, Y. 1993, ApJ, 413, L15
- Keremedjiev, M. & Hao, L. 2006, AAS, 20914912
- Marconi, A., Risaliti, G., Gilli, R., et al. 2004, MNRAS, 351, 169
- McIntosh, D. H., Rieke, M. J., Rix, H.-W., Foltz, C. B., Weymann, R. J. 1999, ApJ, 514, 40
- Netzer, H., Mainieri, V., Rosati, P., Trakhtenbrot, B. 2006, A&A, 453, 525
- Onken, C. A., Ferrarese, L., Merritt, D., et al. 2004, ApJ, 615, 645
- Rekola, R., Riecher, M. G., McCall, M. L., et al. 2005, MNRAS, 361, 330

- Roche, P. F., Packham, C., Telesco, C. M., et al. 2006, MNRAS, 367, 1689
- Sazonov, S., Revnivtsev, M., Krivonos, R., Churazov, E., Sunyaev, R. 2007, A&A, 462, 57
- Shields, J. A. 2007, ASPC, 373, 355
- Shinozaki, K., Miyaji, T., Ishisaki, Y., Ueda, Y., Ogasaka, Y. 2006, AJ, 131, 2843
- Spergel, D. N., Bean, R., Doré, O., et al. 2007, ApJS, 170, 377
- Tully, R. B. 1988, *Nearby Galaxies Catalogue*, Cambridge Univ. Press, New York
- Veron-Cetty, M. P., Veron, P. 2006, A&A, 455, 773
- Wandel, A. 1999, ApJ, 527, 649
- Warner, C. Hamann, F., Dietrich, M. 2004, ApJ, 608, 136